energy.‡ From Eq. (16), it is evident that $g_2(u) = 4\pi[F(x)]^2 \times dF(x)/dx$.

In principle, the expression $g_2(u)$ given in Eq. (20) can now be found. We combine Eqs. (14) and (19) and obtain

$$\int_0^\infty e^{-\beta u} g_2(u)\, du = V(\beta, p) C_1 e^{\beta u_0} \exp[-\{C_2(\ln \beta_o/\beta)^2\}] \quad (20)$$

The inverse transform of the right-hand side of Eq. (20) is $g_2(u)$.

Equations (11) and (19), separately, do not reveal the complete picture. These two equations are connected through Eq. (4); hence the concept of the convolution in Laplace transform theory is pertinent. The product of the two Laplace transforms given in Eqs. (11) and (19) will be called $L_1(\beta)$ and $L_2(\beta)$, respectively. From Laplace transform theory,[5] we have

$$L_1(\beta)L_2(\beta) = \int_0^\infty e^{-\beta E} \int_0^E g_1(E-u) g_2(u)\, du\, dE \quad (21)$$

where $E = \varepsilon + u$. We see that the density of states for a combination of potential and kinetic energy $g(\varepsilon, u)$ is not $g_1(\varepsilon)g_2(u)$ but rather

$$g(\varepsilon, u) = \int_0^E g_1(E-u) g_2(u)\, du = \int_0^E g_1(\varepsilon) g_2(u)\, du = \int_0^E g_2(E-\varepsilon) g_1(\varepsilon)\, d\varepsilon \quad (22)$$

At this time, we shall not attempt to evaluate $g_2(u)$ for argon from the data. We would like to indicate that it can be evaluated from Eqs. (19) and (20). No simple inverse transform of the right-hand side of Eq. (20) is known.

V. Conclusions

In order to utilize inverse relationships, we have determined an analytical form for the partition function for argon gas in the temperature and pressure ranges already specified. Apparently this is the first such listing of an experimental partition function. We find that the partition function for a van der Waals gas inadequate to represent the data. The results tell us that the intermolecular potential for argon gas has a strong repulsive part in the temperature and pressure range under investigation. The equation of state for argon would not reveal the above aspect of the microscopic system. The equation of state could be essentially van der Waals, with the energy aspects of argon being quite different.

The particle partition function is

$$f = (2\pi m/h^2\beta)^{3/2} V_f e^{\alpha\beta} C_1 \exp[-C_2(\ln \beta_o/\beta)^2] \quad (23)$$

which gives the following expression for the equation of state

$$\frac{pV_f}{kT} = V_f \left\{ \frac{1}{V_f} + \beta \frac{\partial \alpha}{\partial V} + \frac{\partial}{\partial V} [\![C_1 \exp[-C_2(\ln \beta_o/\beta)^2]]\!] \right\} \quad (24)$$

The first two terms in the braces constitute the expression for the van der Waals equation of state. If the third term is small, then the equation of state for argon gas is like a van der Waals gas. We did not attempt to investigate the volume (or pressure) dependence of the parameters shown in Eq. (24) and hence can make no remarks in this regard.

References

[1] Din, F., *Thermodynamic Functions of Gases*, Vol. 2, Butterworth, London, 1956.

[2] Eyring, H., Henderson, D., Stover, B. J., and Cyring, E. M., *Statistical Mechanics and Dynamics*, Wiley, New York, 1964, p. 94.

[3] Reif, F., *Fundamentals of Statistical and Thermal Physics*, McGraw-Hill, New York, 1965, p. 426, Eq. (10.5.2).

[4] Robinson, L. B., "Frequency Shifts in the Hyperfine Spectra of Alkalis Caused by Foreign Gases," *Physical Review*, Vol. 117, 1960, p. 1275.

[5] Widler, D. V., *The Laplace Transform*, Princeton Univ. Press, Princeton, N.J., 1946.

‡ Strictly speaking, the right-hand side of Eq. (25) should consist of a linear combination of the types of integral shown. The number of terms is determined by the number of roots of Eqs. (17) or (18). We show only one such term because in the range of temperatures and pressures studied, $\beta U_c(r)$ appears to be a monotone function of r_i.

New Diagnostic Technique for the Study of Turbulent Boundary-Layer Separation

C. C. Horstman* and F. K. Owen†
NASA Ames Research Center, Moffett Field, Calif.

TURBULENT separated flows occur in many types of engineering configurations. They may be unintentional features of some classes of equipment or they may be deliberately introduced. But in all cases such flows can have a significant effect on engineering performance. Furthermore, additional complications are added by the unsteady aspects of the turbulent boundary-layer separation and reattachment processes. Despite the fact that these flows have been extensively studied, detailed information regarding the unsteady nature of turbulent separation is practically nonexistent for high-speed compressible flows. Conventional "time averaged" measurements such as surface pressure, skin-friction, heat-transfer, and pitot pressure surveys cannot supply this information. In this Note, a diagnostic technique is described which provides basic information of the significant unsteady character of turbulent boundary-layer separation. In this technique, thin platinum films are mounted flush with the model surface, and the fluctuating voltages from these films provide measurements related to the flow character above the film. Results are presented for a hypersonic shock-wave turbulent-boundary-layer interaction with and without separation.

The investigation was conducted in the Ames 3.5-ft hypersonic wind tunnel. In this facility, high-pressure heated air flows through the 1.067-m-diam test section to low-pressure spheres. The nominal freestream test conditions were at Mach number 7.2, total pressure of 33 atm, and total temperature equal to 667°K. The test model consisted of a cone-ogive-cylinder, 3-m long and 0.203 m in diameter, with an annular shock wave generator, 0.51 m diam, mounted concentric with the model. The wedge angles of the shock-wave generator were varied from 7.5° to 15° providing a range of shock-wave strengths giving both attached and separated shock-wave boundary-layer interaction flows. The generator was also movable along the cone-ogive-cylinder axis so that the entire interaction region could be passed over a single measurement station on the model. Previous test results[1] without the generator have established the existence of a fully developed, self-similar turbulent boundary layer with negligible pressure gradient from 100 to 300 cm from the model tip. The present measurements were obtained between 180 and 200 cm from the model tip. The measured boundary-layer parameters prior to shock impingement were approximately: edge Mach number of 6.9, boundary-layer thickness of 2.7 cm, Reynolds number based on boundary-layer thickness of 0.2×10^6. The model wall temperature was 310°K. The unsteady aspects of the separated flow region was investigated using thin platinum films deposited on a pyrex glass substrate and mounted flush with the model surface. Gage construction and constant temperature operation were identical to that described in Refs. 2 and 3. The upper frequency limit (−3 db) of the gages, as determined by the conventional square wave technique, was 40 kHz although significant correlations were obtained at frequencies above 65 kHz.

Two typical variations of the rms thin-film voltage fluctuations through the shock-wave boundary-layer interaction region are shown in Fig. 1. Also indicated are the measured pressure

Received March 25, 1974; revision received May 6, 1974.

Index categories: Boundary Layers and Convective Heat Transfer—Turbulent; Supersonic and Hypersonic Flow.

* Assistant Chief, Experimental Fluid Dynamics Branch. Associate Fellow AIAA.

† Consultant; now Senior Research Engineer, United Aircraft Research Laboratories, East Hartford, Conn.

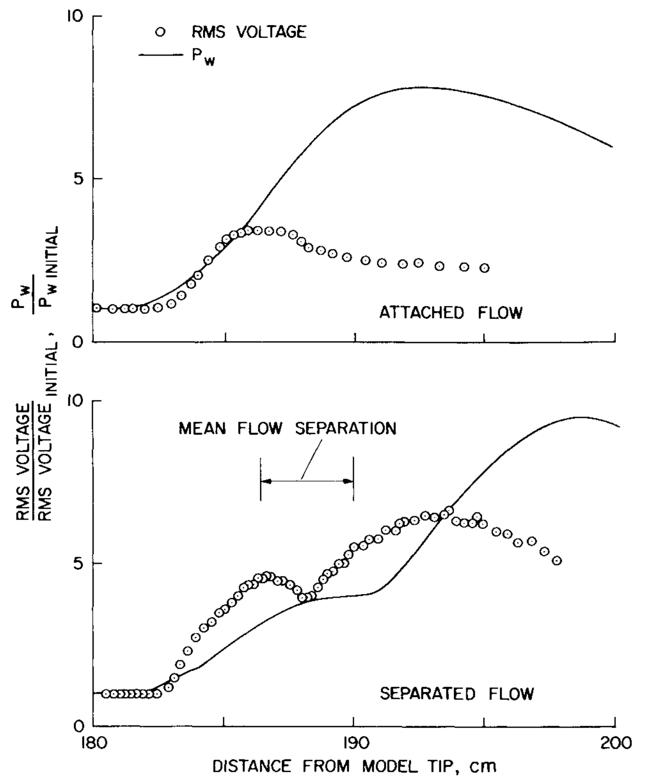

Fig. 1 Normalized rms voltage and surface static pressure distributions for an attached and separated flow.

distributions for the two cases. Data are shown for an attached flow (shock-wave generator wedge angle of 7.5°) and a separated flow (wedge angle of 15°). For both flows detailed pitot pressure surveys, surface skin-friction and surface oil flow data were obtained. These mean measurements indicated attached flow for the 7.5° wedge angle and a substantial region of separated flow for the 15° wedge angle. (The region of measured negative wall shear, as determined from a floating element skin-friction balance, is indicated on the figure.) The thin film results show a marked difference between the attached and separated flows. Normalized power spectra of the fluctuations in the turbulent separated region and after reattachment are shown in Fig. 2 where it can be seen that the energy increase in the separated region is confined to a narrow band around 15 kHz while the increased energy due to the pressure rise after reattachment is broad band. Power spectra containing this energy peak were obtained at measuring stations between 183 and 194 cm from the model tip. Similar measurements were also obtained for the turbulent

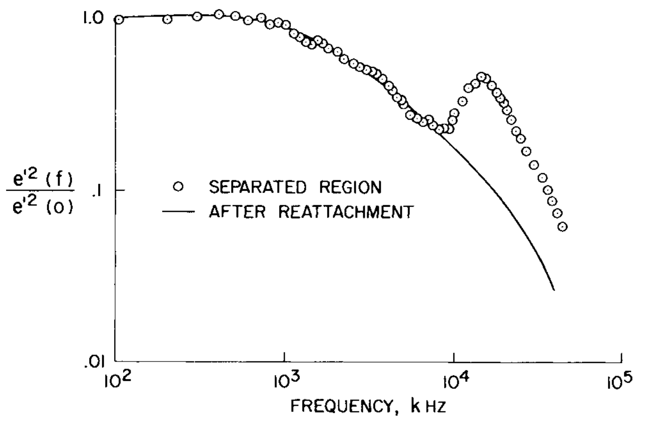

Fig. 2 Normalized energy spectra in the separated region (187 cm) and after reattachment (195 cm).

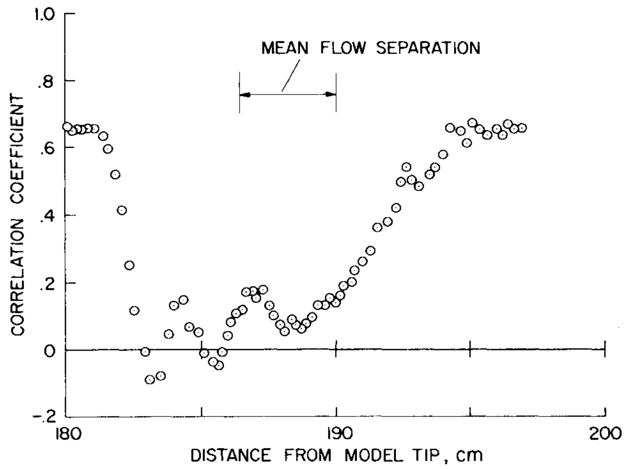

Fig. 3 Optimum correlation coefficient distribution through a separated flow.

attached flow and for a laminar separated flow (at reduced wind-tunnel total pressure). These results showed a smooth power spectra with no energy peak. Since such an energy peak was not evident in these cases, it is felt this peak is associated with turbulent separation unsteadiness. The scale of this unsteadiness, based on measured convection velocities[1] and the measured peak frequency, is of the order of the length of the separated region.

The decrease and subsequent increase in RMS voltage after the first peak for the separated flow (Fig. 1) can also be explained by this unsteadiness. This minimum RMS region, which is where the measured skin friction was most negative, corresponds to the region where the flow remains separated most of the time and least affected by the increased voltage fluctuations due to the unsteadiness of the separation onset and reattachment regions.

Additional measurements of the correlation coefficient between adjacent thin-film gages have also been obtained. This maximum correlation coefficient at optimum time delay through the same separated region for gages spaced 1.5 cm apart is shown in Fig. 3. The correlation coefficient decreases to a value near zero several cm before the time averaged mean flow separated region and increases to the attached boundary-layer value several cm downstream of this region. Data were also obtained for a turbulent attached and laminar separated flows and although the maximum correlation coefficient decreased slightly in the interaction region the only cases where the correlation vanished were for turbulent boundary-layer separations. This is due to the basic unsteadiness of the flow. Verification of this was obtained by measuring several correlation coefficients between adjacent gages using integration times of the order of 0.1 msec. The resulting correlations varied significantly in optimum time delay for maximum correlation. Thus the long time average is low. Indeed, further examination of the simultaneous signals of the two gages on a recording oscillograph indicated turbulence movement both upstream and downstream

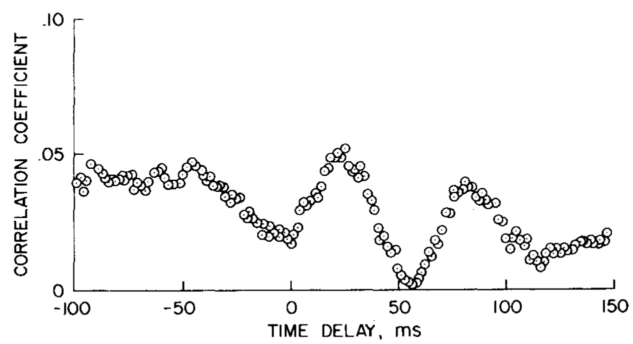

Fig. 4 Typical correlogram in a separated flow region (187 cm).

in the separated region. The frequency of these movements was a maximum near the separation and reattachment points.

Figure 4 shows a typical correlogram in the separated region. This oscillatory nature in the separation bubble is due to the pronounced periodicity shown in Fig. 2.

The length of the separated region as determined by the different measurement techniques varies considerably. The pitot-pressure surveys and surface skin-friction data indicated the shortest region (186–190 cm). Both the surface pressure data (between infection points) and oil flow results indicated a slightly larger region (approximately 184–191 cm). Finally the power spectra and correlation measurements indicated a separated region even greater in extent (approximately 183–194 cm). These results suggest a model for turbulent boundary-layer separation similar to previous incompressible measurements[4]; that is, the onset and reattachment locations of separation are intermittent and only where the flow is reversed at least 50% of the time will the time averaged pitot-pressure and skin-friction measurements indicate separated flow while the instantaneous thin-film measurements are sensitive to regions which are separated for only a small fraction of time.

References

[1] Owen, F. K. and Horstman, C. C., "On the Structure of Hypersonic Turbulent Boundary Layers," *Journal of Fluid Mechanics*, Vol. 53, June 1972, pp. 611–636.

[2] Owen, F. K., "Transition Experiments on a Flat Plate at Subsonic and Supersonic Speeds," *AIAA Journal*, Vol. 8, No. 3, March 1970, pp. 518–523.

[3] Owen, F. K. and Horstman, C. C., "Hypersonic Transitional Boundary Layers," *AIAA Journal*, Vol. 10, No. 6, June 1972, pp. 769–775.

[4] Sandborn, V. A. and Liu, C. Y., "On Turbulent Boundary-Layer Separation," *Journal of Fluid Mechanics*, Vol. 32, May 1968, pp. 293–304.

Stability of Flow through Porous Plates: Coalescent Jets Effect

MARCOS PIMENTA* AND ROBERT J. MOFFAT†
Stanford University, Stanford, Calif.

Introduction

THE main purpose of our experiments has been the study of turbulent boundary-layer development over smooth or rough porous plates with transpiration. Special treatment is given to heat-transfer studies, partly motivated by the current interest in protecting surfaces from hot streams in combustion chambers, turbines, and other applications.

During the qualification runs of the recently completed HMT apparatus for roughness studies, tests were conducted to determine the uniformity in porosity of the plates. These tests showed anomalous results: the flow through the plates seemed to coalesce into definite jets rather than come through the plate in a uniform manner. It was feared that this jetting action could appear even in the presence of a shear flow and have some effect on our boundary-layer heat-transfer measurements. This, in fact, motivated a more detailed analysis.

As it has been pointed out earlier by several authors, the flow through porous screens can under certain conditions present instabilities. A similar result has been observed for flow through permeable plates. In our present experiment, two different plates were investigated, both constituted of small spheres stacked in the densest arrangement and sintered together. One with 0.005-in.-diam spheres and the other, 0.050-in.-diam spheres. The main feature of the flow is the formation of jets leaving the surface which coalesce with each other in a spatially random but repeatable manner. This phenomenon occurs once the air leaving the porous surface exceeds a certain critical velocity. A quasi-hysteresis effect has also been observed. Once the jets have coalesced, their pattern is preserved even at air surface velocities smaller than the critical velocity. The plate made of the smaller particles has a larger critical velocity and a much finer jet pattern. Finally, it has been determined that the heat transfer from the plates to a free-stream flowing over them is not enhanced when the transpiration surface velocity exceeds the critical velocity. This observation suggests that the shear flow over the plates may stabilize the jets, preserving a uniform transpiration to a much higher value of velocity.

Received March 15, 1974; revision received June 3, 1974.

Index categories: Boundary Layers and Convective Heat Transfer—Turbulent; Jets, Wakes, and Viscid-Inviscid Flow Interactions.

* Graduate Student, Department of Mechanical Engineering.

† Professor, Department of Mechanical Engineering.

Previous Works

Most existing reports of flow instabilities behind porous surfaces refer to two-dimensional flows behind screens and rod grids. By flow instability, we mean here the coalescence of jets behind the porous surface. The first experimental work was presented by MacPhail.[1] In his case he was interested in solving the problem of obtaining a uniform velocity distribution in a duct downstream of a 90° bend followed by a sudden expansion.

An experimental investigation carried out by von Bohl[3] studied the stability behind a grid of rods in a closed duct. His main conclusion was that, depending on the open area ratio of the grid, he was able to get stable and unstable flows. The study by von Bohl showed that open ratios of 0.63 and 0.54 corresponded to stable and unstable conditions, respectively.

Corrsin[4] also reports a study on the stability of two-dimensional flow through a grid of rods with an open area ratio of 0.17. He observed unstable flow so irregular that sufficiently far from the grid one could not see any evidence of the flow coming from a regular row of jets. His main interest was also, primarily, in a way of controlling it and overcoming the instability.

Finally, Bradshaw,[5] in a more recent paper, describes the nonuniformity problem that he obtained in a spanwise shear stress distribution in a two-dimensional wind tunnel. As he states, the last wire mesh screen of the tunnel screen arrangement was responsible for the nonuniformity. He concluded that a 0.57 open ratio is the minimum value to avoid instability. He also suggests a minimum distance between screens.

Morgan[2] and Bradshaw[5] attribute the cause of the instabilities to the coagulation of the jets coming out from the screens, which in its turn depends upon the entrainment of air by individual jets from the wakes between them. A critical open area ratio does exist, below which the entrainment is so large that different jets coalesce together.

Besides these references, very few authors report studies for the three-dimensional case. Morgan[2] refers to perforated plates for which he says there is no critical open area ratio. For the same case as Bradshaw, i.e., wire screen, he mentions a critical ratio of 0.5.

Schubauer[6] mentions that the coalescence of jets in certain circumstances for open area ratios of less than 0.5 can cause spatial variations in velocity as well as a higher turbulence level.

Present Investigation

Our present investigation was done using two of the Stanford HMT group wind tunnels. Both have been designed for turbulent boundary-layer studies with transpiration (for description of apparatus, see Ref. 7). The one reserved to smooth plate studies has 24 porous plates made from 0.005-in.-diam particles, the other, for roughness-effect studies, has 24 porous plates made from 0.050-in.-diam spheres sintered together.